SCIREA Journal of Mechanical Engineering
ISSN: 2995-7729
http://www.scirea.org/journal/Mechanical
April 1, 2024
Volume 5, Issue 1, February 2024
http://dx.doi.org/10.54647/mechanical460108

Design and experimental study of Mechanical Milling deicing device

Yan Diao [1]

[1] China Heavy Truck Group Co.,Ltd,Jinan,Shandong,250116,China

Email:1737859521@qq.com (Yan Diao)

Abstract

To quickly and economically remove the accumulated ice and snow on airport runways, urban roads and bridge decks is an important subject to ensure smooth traffic and driving safety under the condition of snow and ice climate. Based on analysis of different mechanical deicing techniques and the combination of thermal and water jet cutting deicing methods, a mechanical milling deicing method was proposed. Through the establishment of a milling deicing cutting model and the force analysis of the deicing cutter, the optimal deicing angle of the milling cutter was obtained, and the rationality of the design of the milling deicing cutter was verified based on ANSYS. The feasibility of the design scheme is verified by the test of mechanical milling deicing device.

Key words: Milling deicing device; Deicing knife tool; ANSYS; Experimental study

1. Introduction

Every winter, many areas are often hit by ice and snow, resulting in the reduction of the

friction coefficient of the road surface, making the vehicle driving, braking difficulties or skid, easy to cause traffic accidents, to people's lives and property brought serious losses（Zicheng Zhu and Xuejun Zhang ,etal.2015）. At present, commonly used mechanical deicing methods can be divided into brush type, shovel type, rotary cutting type, shovel type and so on (HU Z D and DU S R ,etal.2015). Operational efficiency of brush deicing is relatively low, and the application scope is narrow. Soft brush can only be used to remove snow float, while stiff brush can only be used to remove snow and ice with high hardness, and it is easy to cause damage to the road surface during operation(Wang Feng and Jing Hongjun 2022).Shovel scraper deicing is highly efficient in the operating environment where the road surface is flat and the road surface has minimal adhesion(Zhang Hongfang and LuShan,etal.2020). However, compaction snow and thawing snow and ice have excellent resistance to shovel scraping, so the thickness of snow and ice removal is limited (Wang Z and Zhang T, etal.2017). Rotary cutting deicing is driven by the driving device to rotate the roller, and the helical teeth or ruler on the roller is relatively compacting snow or thawing snow and ice for milling and milling, so that the hard snow and ice on the road surface are broken and then removed, but its shovel edge wears fast, and it also has a certain destructive effect on the road surface. Shovel and chop deicing is only suitable for snow and ice removal operations of medium density, and the operational efficiency is low, and the snow and ice residue on the road is obvious, which is not suitable for high-speed operation. If the adjustment of the chop force is not appropriate, it is easy to damage the road. Therefore, the application scope of the shovel and chop ice and snow clearing equipment is limited(Wang Yongfeng and Wang Lizhi 2018).

Considering the advantages and disadvantages of the deicing method, combined with the heat and water jet cutting and deicing method, this paper proposes and designs a kind of mechanical road surface milling deicing device, establishes the milling deicing model, carries out the force analysis of the deicing tool, obtains the best deicing tool of the device, and carries out the feasibility test.

2. Structure and working principle of milling deicing device

Mechanical milling deicing device is composed of a milling deicing cutter, a driving motor, a pilot wheel and its linkage mechanism (as showed in Fig.1). In the deicing operation, the driving motor drives the deicing cutter to carry out the deicing operation. The pilot wheel can track the high and low undulation of the road surface in real time, and adjust the height of the

deicing tool with the linkage mechanism between the pilot wheel and the mechanical deicing tool. On the premise of guaranteeing the quality of deicing, it can avoid the contact between the tool and the road surface, so as to protect the tool.

Fig.1. Mechanical milling deicing device: (a) Three-dimensional design model; (b) Entity structure

3. Structure analysis and optimization design of mechanical milling ice cutter

3.1 Cutting force model and force analysis of milling deicing

3.1.1 Cutting force model of milling deicing

During milling and deicing operations, the force on the deicing device is the spatial force (FIG. 2 and 3), which is composed of three components: Fc tangential milling component, Fr radial milling component and Fz axial milling component. In the process of milling deicing, the cutting force of the main cutting edge can be ignored because the cutting feed of the main cutting edge and the auxiliary cutting edge are small and the participating length of the auxiliary cutting edge is slight.

The tangential milling component Fc, radial milling component Fr and axial milling component Fz are expressed as:

$$F_c = p \cdot a_p \cdot f_z \cdot \sin\varphi \tag{1}$$

$$F_r = \eta' F_c = \eta' \cdot p \cdot a_p \cdot f_z \cdot \sin\varphi \tag{2}$$

$$F_z = \eta' \cdot \cot k_r \cdot F_c = \eta' \cdot \cot k_r \cdot p \cdot a_p \cdot f_z \cdot \sin\varphi \tag{3}$$

In the formula, a_p — milling depth (mm);

p — Unit cutting force (N/mm^2);

f_z — Feed per tooth (mm/z);

φ — Feed direction Angle (°);

k_r — Tool main deflection Angle (°);

η' —Coefficient, related to milling conditions, cutting Angle, cutter sharpness and feed to change.

In the process of milling deicing, the cutter's tangential milling component Fc is the largest in the cutting force, so it is considered as the main cutting force.

3.1.2 Force analysis of milling tool

According to the anti-interference milling theory(Zhu Haoran and Yu Mingming,etal.2019), the tool force analysis diagram showed in Fig. 2 and the velocity vector synthesis diagram of tool tip point A shown in Fig. 3 are established, and the following results are obtained:

$$\tan\beta = \frac{2\pi nr\sin\theta_i}{1000v + 2\pi nr\cos\theta_i} \tag{4}$$

$$W = \frac{1000vt_1}{60} \tag{5}$$

$$\frac{a_e}{\sin\beta} = \frac{W}{\sin[\pi - (\alpha - \beta)} \tag{6}$$

According to formula (4), (5) and (6), the thickness formula of milling deicing can be obtained:

$$a_e = \frac{W\sin\beta}{\sin[\pi - (\alpha - \beta)]} \tag{7}$$

$$\alpha = \frac{\pi}{2} - \theta_i - \lambda \tag{8}$$

In the formula, n—Milling cutter head speed（nim^{-1}）；

V—0perating speed（m/s）；

t_1-The time it takes the knife to circle（s）；

r—Radius of milling（mm）；

λ—Angle of invasion（^{o}）；

θ_1—Corresponding point milling cutter head Angle（^{o}）；

β—The Angle between the absolute speed of the tip and the ice（^{o}）；

α—Angle between the axis of the cutter head and the horizontal plane（^{o}）。

Thus, the calculation formula of cutting tool milling deicing resistance is:

$$F_w = \frac{k_w B a_e v}{u} = \frac{k_w B v}{R\omega} \bullet \frac{W \sin\beta}{\sin[\pi-(\alpha-\beta)]} \tag{9}$$

In the formula: k_w —resistance coefficient (1.2×105);

B —milling width (take 200mm);

a_e—Milling thickness (mm);

u—Milling cutter head linear speed(mm/s);

ω— Angular speed of milling cutter head (rad / s).

It can be concluded that:

$$F_W = 4\times10^3 \bullet \frac{v\sin\beta}{\sin[\pi-(\alpha-\beta)]} \tag{10}$$

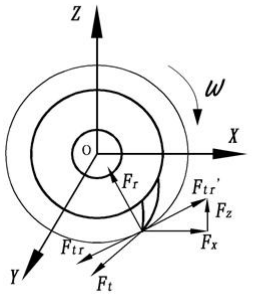

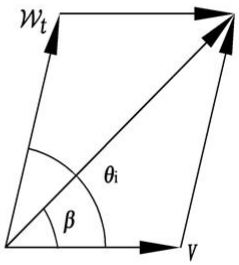

Fig.2. Cutting tool force analysis **Fig.3.** Velocity vector synthesis diagram of tool tip

3.2 Selection of milling tool Angle

The front angle (γ)of the deicing cutter is the angle between the base surface and the front cutter surface, which affect the shape of the milling ice chip. The back angle (α)is the Angle between the milling plane and the back cutter surface, which affects the friction between the ice cutter and the ice. The angle between the front blade and the back blade is the wedge

angle(β), which is the main factor affecting the strength and sharpness of the deice cutter. The angle between the milling plane and the front cutter face is the milling angle(δ), which reflects the tilt degree of the front cutter facing the milling plane(Fig.4). Each Angle satisfies the following relation:

$$\alpha + \beta + \gamma = 90^0 \tag{11}$$

$$\delta = \beta + \alpha = 90^0 - \gamma \tag{12}$$

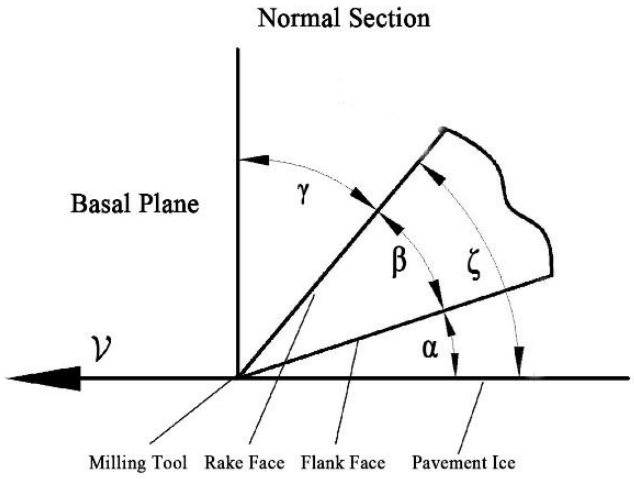

Fig.4. Angle diagram of de-icing tool

After the selected cutter is determined, the size of the back Angle α determines the deicing effect of milling. In order to select the best back Angle α and verify the feasibility of the scheme, a simple milling deicing device was made, and corresponding verification tests were carried out. The test results are given in table 1. According to the data in the table, when the rear angle is between 5 and 10^0, the average thickness of road residual ice is the minimum and the deicing effect is the best.

Table 1. Different Rear Angle Test Data

Back Angle α /^{0}	Forward Velocity m/s	Pavement Residual ice Thickness mm
0~5	0.2	1.45
5~10	0.2	1.05
10~15	0.2	1.34
15~20	0.2	1.73

3.3 Milling tool simulation analysis

When stimulated by external conditions, the mechanism often produces resonance. During the resonance, the amplitude of the mechanism increases obviously and the excitation force is enhanced, which makes the mechanism produce large deflection and accelerate the damage rate. Therefore, it is necessary to examine the vibration problem when designing the cutter of milling deicing device.

3.3.1 Establishment of tool model

According to the operation requirements of the milling deicing device, the relevant data of the cutter head design are as follows: the cutter head diameter is 200mm, the wall thickness is 10mm, the tooth body and the middle hole diameter is 10mm, the number of teeth is 16, and the material density $\rho = 7.8\times10^{3} kg/m^{3}$, modulus of elasticity E= $2.06\times10^{11} Pa$, poisson's ratio was 0.3.The three-dimensional solid model of the parametric was constructed by Creo Parametric, as showed in the Fig.5.

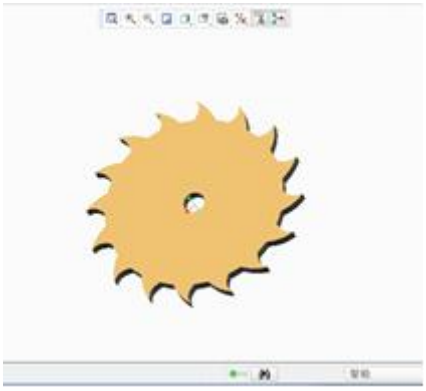

Fig.5. 3D model of tool

Block Lanczos algorithm was used to set the order of mode extraction as 15, and the first 15 orders of natural frequency, mode shape and amplitude changes were calculated as showed in the Fig.6. As can be seen from the figure, the first six natural frequencies are relatively small, close to 0. From the 7th order, the natural frequency gradually increases from 2.0616Hz to 8.846Hz at the 15th order. In practice, it is almost impossible to make the applied excitation frequencies completely avoid these natural frequencies. Therefore, we can only discuss the natural frequency interval of the minimum amplitude by combining the mode diagram.

SET,LIST Command

File

***** INDEX OF DATA SETS ON RESULTS FILE *****

SET	TIME/FREQ	LOAD STEP	SUBSTEP	CUMULATIVE
1	0.0000	1	1	1
2	0.0000	1	2	2
3	0.0000	1	3	3
4	0.51917E-05	1	4	4
5	0.21422E-04	1	5	5
6	0.32554E-04	1	6	6
7	2.0616	1	7	7
8	2.2187	1	8	8
9	3.4764	1	9	9
10	4.8022	1	10	10
11	4.8867	1	11	11
12	7.0062	1	12	12
13	7.2745	1	13	13
14	8.3733	1	14	14
15	8.8469	1	15	15

Fig.6. 15 orders of natural frequency

3.3.2 Analysis of tool simulation results

It can be seen from the Fig.7 that the amplitude of modes of order 1 to 6 is small. The maximum shape variable is 0.54mm, and the natural frequency is basically zero. Where, at order 1, order 3 and order 4 natural frequencies, the cutter head swings up and down with XOY as the center plane; At the second order natural frequency, the tool coil rotates and vibrates around the Z axis. At order 5 and 6 natural frequencies, the cutter head swings up and down with YOZ as the center plane.

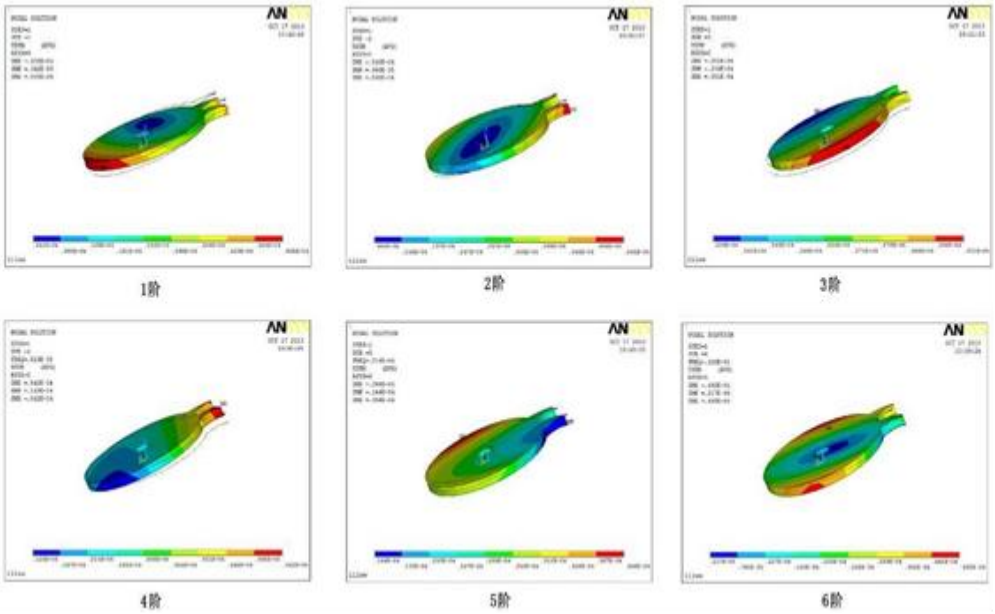

Fig.7. 1~6 order natural frequency

At the 7th order natural frequency, the cutter head takes YOZ plane as the center plane, and both sides of the cutter head bend towards YOZ plane, with the maximum deformation of 0.865mm. Under the 8 order natural frequency, the cutter head is centered on XOZ plane and

YOZ plane respectively, and the outer side of the cutter head is bent to the center plane. The maximum deformation is located on the outer side of the cutter head disk and the edge of the mechanical rotary cutting edge, about 0.601mm. At the 9th-order natural frequency, the mode shape of the cutter head is more complex, bending toward the center of the cutter head in an umbrella shape, and the maximum deformation is located at the tip of the mechanical rotary cutting edge of the gear teeth, about 0.820mm. At the natural frequency of order 10, the mode shape of the cutter head is opposite to the bending direction of order 9, and it is still umbrellalike, and its maximum shape variable is 1.540mm (Fig.8).

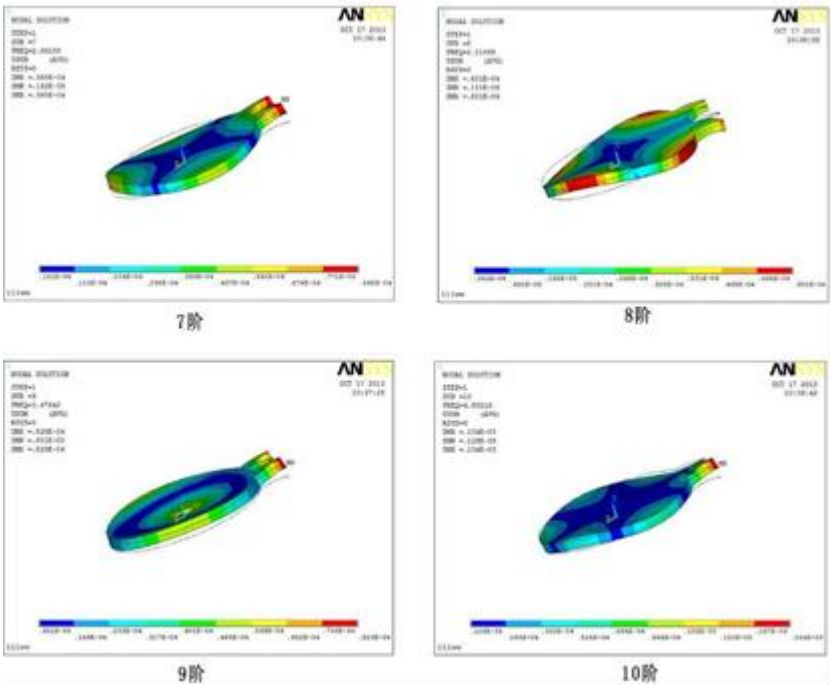

Fig.8. 7~10 order natural frequency

The natural frequency of order 11 ~ 14 varies from 4.8867Hz to 8.3733Hz, and the range of variation is also expanded. The shape is shown as follows(Fig.9): at the natural frequency of order 11, the cutter head is centered on the XOY plane, and the top of the gear teeth vibrates up and down in it. The maximum shape variable is 1.33mm. The modes of order 12 and order 13 are similar. They vibrate up and down along XOY as the center plane and bend along YOZ plane, respectively. The maximum shape variable is 2.32mm. The 14th order mode is slightly simpler and its shape variable is smaller, 0.659mm. Fig.10 shows the 15 order mode of the cutter head. As can be observed in the figure, the vibration of the cutter head is relatively stable. From the mechanical rotary cutting edge to the edge of the cutter head, the resonance is performed along the central plane of XOY, and the amplitude is small. The maximum deformation is 0.9mm.

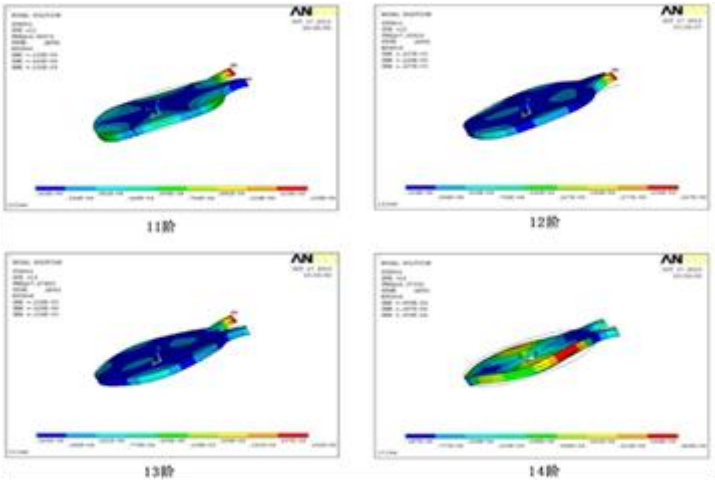

Fig.9. 11~14order natural frequency

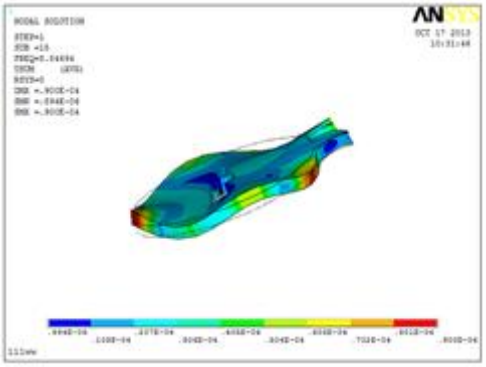

Fig.10. 15 order natural frequency

According to Von Mises equivalent stress nephograph in Fig.11, it can be seen that the stress concentration phenomenon of the deglaciator tool is very rare and only exists in the root part of the mechanical rotary cutting edge.

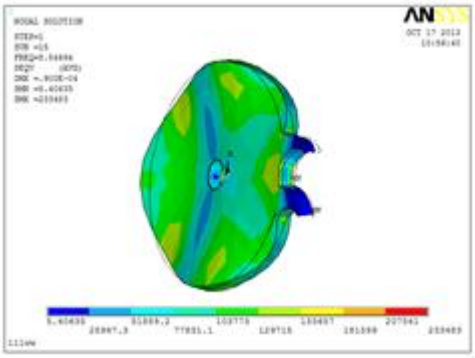

Fig.11. Von Mises equivalent stress nephograph

3 Test analysis of milling deicing device

According to the above theoretical analysis and experimental research, in order to verify the

feasibility of the device, mechanical milling and deicing device for road surface were designed and made (Fig.12). A driving motor with a power of 1450W and a speed of 13000r/min was selected, and a woodworking saw blade with a diameter of about 20cm commonly used in the market was selected as the deicing tool. The corresponding deicing operation test was carried out in the indoor low-temperature laboratory, and the test data were accounted for and analyzed (Fig.13, Fig.14).

Fig.12. Milling deicing mechanism test prototype

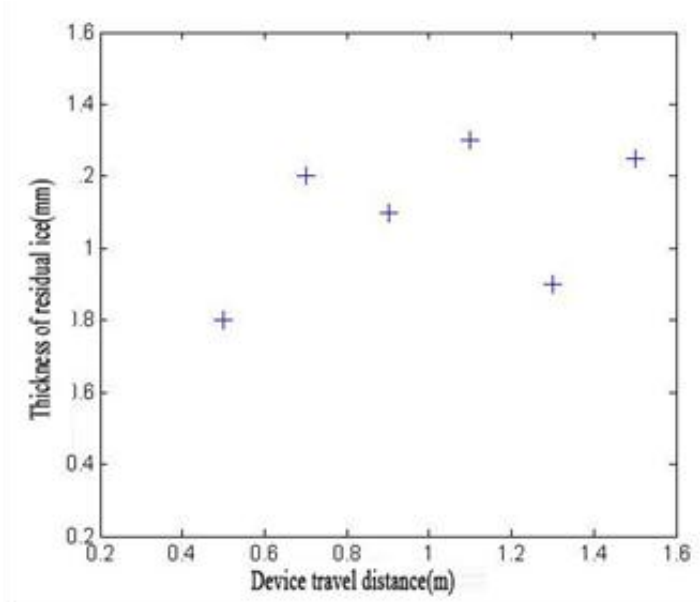

Fig.13 Milling deicing test data

Fig.14. Milling deicing effect

4 Conclusions

The mechanical deicing device was designed by using the mechanical milling method, and the cutting model of the deicing cutter was established. Force analysis of the deicing cutter was carried out, and the optimal deicing angle of the milling cutter was obtained (the back angle was 5~10^0). The ANSYS finite element simulation analysis showed that the deicing cutter had very little stress concentration phenomenon and the structure was stable. The milling deicing test proves that the milling deicing device can comply with the requirements of deicing operation and work stably and reliably. The milling deicing device is further combined with the thermal melting deicing device, which can realize the complementary advantages, small damage to the road surface, economic and environmental protection, and can better complete the task of road surface deicing.

References

[1] Zicheng Zhu, Xuejun Zhang , Qiang Wang ,Weijun Chu ect. Research and Experiment of Thermal Water Deicing Device[J]. Trans. Can. Soc. Mech. Eng. 2015,39(4):783-788.

[2] HU Z D，DU S R，SHEN B C,et al.Mechanical property analysis on cutting tool of the ice

and sn IW removmg machine based on ansys[J]. Applied Mechanics &Ma - terials,2015,779 :74-79.

[3] Wang Feng,Jing Hongjun,SongMei ect. Modified magnesium oxychloride cement aggregate and its self-snowmelt performance [J]. JOURNAL OF XI' AN UNIVERSITY OF SCIENCE AND TECHNOLOGY. Vol.42, No.5, 2022.

[4] Zhang Hongfang and LuShan, et al. Tem- poral and spatial distribution characteristics of road icing in Shaanxi and its risk warning model[J]. Drought Weather,2020,38(5):878-885.

[5] Wang Z, Zhang T, Shao M, et al. Investigation on snow-melting performance of asphalt mixtures incorporating with salt-storage aggregates [J]. Construction and Building Materials,2017,142 (7) :187-198.

[6] WANG Yongfer, WANG Lizhi. Ice suppression and skid resistance of composite salt storage asphalt tmixture [J]. Road Construction Machinery and Construction Mechanization201835(6) :69-72.

[7] ZHU Haoran,YU Mingming,WEN Xiaobo. Experimental study on properties of slow-re1ease snow and ice prevention materials [J]. Journal of Chongqing Jiaotong University(Natural Science Edition) .2019,38 (4) :66-71.

[8] Jianzhao Zhou, Siwei Lai, Xiaopan XU, Yunhe Chen, Weijun Chu, Yaming Gao, “R&D of Equipment for Deicing by Thermal Water-jet and Mechanical Deicing Method”, IEEE Int. Conf. on Applied Mechanics, Materials and Manufacturing, Changchun, China, 1288~1293 November(2012).

[9] ZHOU Jianzhao, LI Cong, CHU Weijun, et al. R&D of Vehicle for De-Icing Quickly by Thermal and Water Jet on the Pavement[J] . Machinery design & Manufacture,2012,（8）：113-115.

[10] ZHU Zicheng, ZHANG Xuejun, et al. Research of Rapid Compound Deicing Equipment[J]. Machine Tool ＆ Hydraulics,2014,42(8):16-19.